ELSEVIER

Journal of Chromatography A, 691 (1995) 171–185

JOURNAL OF CHROMATOGRAPHY A

Solvent modulation in liquid chromatography: extension to serially coupled columns

Patrick H. Lukulay, Victoria L. McGuffin*

Department of Chemistry, Michigan State University, East Lansing, MI 48824-1322, USA

Abstract

The concept and theory of solvent modulation are extended to serially coupled columns in liquid chromatography. Because the mobile phases are maintained in separate zones and the stationary phases in separate columns, solute retention is a simple, time-weighted average of the individual environments to which the solute is exposed. Thus, optimization of complex multidimensional chromatographic separations is more accurate and predictable. This approach is demonstrated by application to the separation of isomeric polynuclear aromatic hydrocarbons using octadecylsilica and β-cyclodextrin silica stationary phases with aqueous methanol and acetonitrile mobile phases.

1. Introduction

Liquid chromatography has gained acceptance as the method of choice for the separation of complex mixtures of non-volatile solutes. Solute retention and selectivity are controlled by the physical and chemical properties of both the stationary and mobile phases. In general, optimization is performed in two successive stages: a coarse adjustment is achieved by selection of the appropriate stationary phase(s) and a fine adjustment by means of the mobile phase(s), whose composition can be more readily varied [1,2].

A variety of methods has been developed to optimize the strength and selectivity of the mobile phase. In most of these methods, a preliminary series of experiments is performed to measure solute retention in mobile phases of known composition. From these measurements, the optimum composition for isocratic or gradient elution is predicted by using a predefined mathematical function [3–8]. On the basis of thermodynamic considerations, solute retention is generally considered to be a linear or quadratic function of the composition of the mobile phase [7–9]. This presumption implies that the solute interacts independently with each solvent component of the mobile phase. Unfortunately, molecular interactions are not completely independent of one another in water and many polar organic solvents [10]. This non-ideal behavior limits the accuracy and precision with which solute retention may be predicted using linear or quadratic models [7,11].

To enable the solute to interact independently with each solvent component, several workers have investigated the introduction of the mobile phase as separate zones onto the chromatographic column. Berry [12] has developed a method in which one or more zones of a weak eluent, typically water, are strategically timed to arrive at a pair of unresolved solutes and facilitate their

* Corresponding author.

0021-9673/95/$09.50
SSDI 0021-9673(94)01184-2

separation. Berry et al. [13,14], Gluckman et al. [15], and Little et al. [16] have demonstrated that several zones with different elution properties, such as pH, ion pairing, and hydrophobic interactions, may be used to resolve strong and weak acids and bases as well as neutral solutes. More recently, Wahl et al. [17–19] have generalized this concept and theory for multiple solvent zones that are applied to the column in a random or repeating sequence. Because the solvent zones are spatially and temporally separated, solute retention is controlled independently within each zone. Therefore, the overall retention is a simple time-weighted average of the solute capacity factors in the individual solvent zones. This technique, known as solvent modulation by Wahl et al. [17–19], appears to provide a versatile alternative to premixed mobile phases for the rapid and accurate optimization of separations.

In addition to optimization strategies for the mobile phase, stationary phase optimization has also been implemented to resolve complex mixture of solutes. When a single stationary phase is not sufficient, mixed or multimodal stationary phases have been used to combine dissimilar but compatible retention mechanisms. Mixed phases that have been successfully used include reversed-phase with size exclusion [20–23], cation or anion exchange with size exclusion [23], reversed-phase with cation or anion exchange [24–28], and cation with anion exchange [27,29]. These stationary phases may be combined in several ways: by incorporating or chemically bonding the stationary phases on the same particles (chemically mixed support), by incorporating the phases on different particles that are mixed within a single column (physically mixed support), or by incorporating the phases on different particles that are contained in separate columns connected in series [28]. Isaaq et al. [22] observed that solute retention on chemically or physically mixed supports may not be predictable as a linear function of the stationary phase composition. This non-linear additivity of solute retention may arise as a consequence of interactions between the different stationary phases. On the other hand, retention on serially coupled columns is generally additive and predictable because the stationary phases are physically separated.

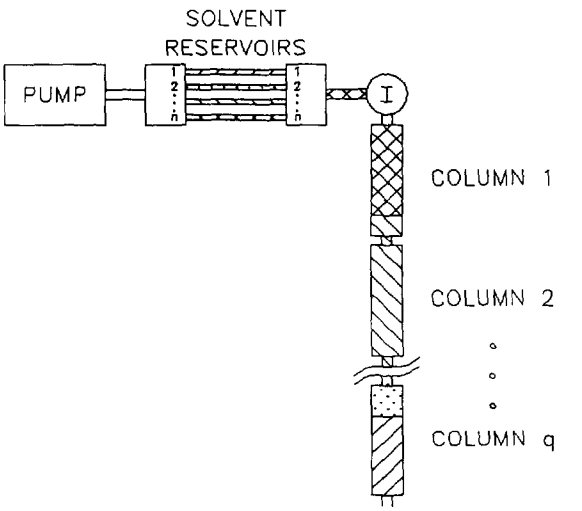

Fig. 1. Schematic illustration of n solvent zones in q serially coupled columns.

In this work, the use of serially coupled columns and solvent modulation is investigated as a viable strategy for the optimization of both stationary and mobile phases. By maintaining the stationary phases in separate columns and the mobile phases as separate zones, the solute will interact independently in each environment (Fig. 1). Thus, overall solute retention will be a simple, predictable function of the capacity factor weighted by the time that the solute is exposed to each stationary and mobile phase. This approach should allow accurate prediction of solute retention and, hence, allow optimization of multidimensional separations with a minimum number of preliminary experiments.

2. Theory

2.1. Theory of solute retention

In order to optimize separations on serially coupled columns under the conditions of solvent modulation, the theoretical basis of retention must be established. The inherent assumption underlying this theory is that solute retention is controlled independently within each solvent zone. In addition, it is assumed that the column is able to achieve steady-state conditions rapidly

after each change of solvent. This latter requirement may restrict the selection of both mobile and stationary phases. The validity of these assumptions has been demonstrated previously for a single column [17,18], and is extended here for serially coupled columns.

The capacity factor (k_{ijp}), which is the thermodynamic measure of solute retention, may be expressed as follows:

$$k_{ijp} = \frac{t_{ijp}}{t_{ojp}} - 1 \tag{1}$$

where t_{ijp} and t_{ojp} are the elution time of a retained and a non-retained solute, respectively, in solvent j and on column p. It may be readily shown [17,30] that the residence time of a solute in a solvent zone of length x_j is given by:

$$t_{ijp} = \frac{x_j}{u_p}\left(\frac{1 + k_{ijp}}{k_{ijp}}\right) \tag{2}$$

where u_p is the mobile phase linear velocity on column p. The total retention time (T_i) of the solute is the summation of residence times in each solvent and on each column

$$T_i = \sum_{p=1}^{q}\sum_{j=0}^{n} t_{ijp} = \sum_{p=1}^{q}\sum_{j=0}^{n} \frac{x_j}{u_p}\left(\frac{1 + k_{ijp}}{k_{ijp}}\right) \tag{3}$$

Because the volumetric flow-rate (F) of the mobile phase remains constant within the chromatographic system, the linear velocity on each column is related by

$$F = \pi r_p^2 \varepsilon_p u_p \tag{4}$$

where r_p is the radius and ε_p is the total porosity of column p. By rearrangement of Eq. 4 and substitution into Eq. 3, the total retention time may be expressed in terms of the known column parameters

$$T_i = \sum_{p=1}^{q}\sum_{j=0}^{n} \frac{\pi r_p^2 \varepsilon_p x_j}{F} \cdot \left(\frac{1 + k_{ijp}}{k_{ijp}}\right) \tag{5}$$

The limit of the summation index (n), which represents the total number of solvent zones required to elute the solute from a column of length l_p, is determined by evaluating the expression

$$\sum_{j=0}^{n} \frac{x_j}{k_{ijp}} = l_p \tag{6}$$

If the limit has a non-integer value for the first column ($p = 1$), the summation in Eq. 5 is performed in the normal manner for the integer solvent zones 0 to n, and the fraction is treated as a multiplier for the last solvent zone. This solvent zone subsequently enters the second column, where the remainder is used as a multiplier for the first solvent zone ($n = 0$) on the second column ($p = 2$). The computation is performed in an analogous manner for all subsequent columns.

2.2. Theory of solute band broadening

In order to optimize the separation of solutes on serially coupled columns, the variance of the solute peak must be determined at the exit of the last column. If the broadening arises primarily from the packed bed and is relatively independent of solute and solvent, the variance in length units $(\sigma_{ijp})_l^2$ can be expressed as:

$$(\sigma_{ijp})_l^2 = h_p d_p l_p \tag{7}$$

where h_p is the reduced plate height, d_p is the particle diameter, and l_p is the length of column p. Since variances are only independent and additive in the time domain [31,32], the length variance within each solvent zone on each column must be converted to the corresponding temporal variance $(\sigma_{ijp})_t^2$

$$(\sigma_{ijp})_t^2 = \frac{(\sigma_{ijp})_l^2}{u_p^2} \cdot \left(\frac{t_{ijp}}{t_{ojp}}\right)^2 \tag{8}$$

where the elution time of a retained solute is given by Eq. 2 and the elution time of a non-retained solute (t_{ojp}) is given by

$$t_{ojp} = \frac{l_p}{u_p} \tag{9}$$

By substitution of these expressions into Eq. 8, the total temporal variance can be expressed as a summation of the contributions within all solvent zones and all columns

$$(\sigma_t)_t^2 = \sum_{p=1}^{q}\sum_{j=0}^{n}(\sigma_{ijp})_t^2 = \sum_{p=1}^{q}\frac{h_p d_p}{l_p} \cdot \left[\sum_{j=0}^{n}\frac{\pi r_p^2 \varepsilon_p x_j}{F}\cdot\left(\frac{1+k_{ijp}}{k_{ijp}}\right)\right]^2 \quad (10)$$

Finally, the effective number of theoretical plates (N) for the coupled column system under the conditions of solvent modulation is given by

$$N = \frac{T_i^2}{(\sigma_t)_t^2} \quad (11)$$

where the total retention time and temporal variance are evaluated from Eqs. 5 and 10, respectively.

2.3. Theory of solvent zone broadening

In order to ensure that solute retention is controlled independently within each solvent zone, it is necessary that the zones exhibit minimal mixing at the boundaries. Such mixing will adversely influence the accuracy of predicting solute retention from the theoretical models. Moreover, distortion and even splitting of solute peaks may occur if they elute at or near the solvent zone boundary.

The zone purity can be expressed as the ratio of the lengths of the unmixed fraction of the final solvent zone to that of the original zone

$$\frac{x_j - \xi x_j}{x_j} = 1 - \xi \quad (12)$$

When defined in this manner, the zone purity approaches unity when no intermixing occurs and approaches zero when the solvent zone is completely mixed by column broadening processes.

Determination of the zone purity by means of Eq. 12 requires an estimation of the mixed fraction (ξ) of the solvent zone. This mixed fraction may be estimated by assuming that the initial solvent zone has an ideal rectangular profile of width x_j and that column broadening processes are adequately described by a Gaussian profile with variance given by Eq. 7, as illustrated schematically in Fig. 2. The mixed fraction is then calculated, with a statistical accuracy of 95%, by presuming that mixing extends $2(\sigma_o)_l$ at each boundary of the solvent zone, so that the total mixed region is $4(\sigma_o)_l$. The mixed fraction is, thus, given by

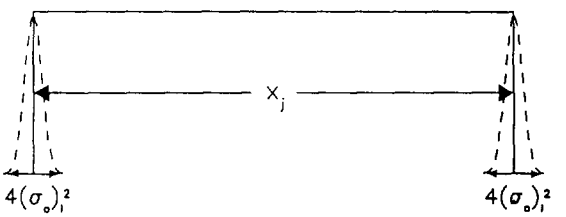

Fig. 2. Schematic illustration of solvent zone broadening ($1 - \xi = 0.95$).

$$\xi = \frac{4(\sigma_o)_l}{x_j} \quad (13)$$

where the total variance for a non-retained solvent zone $(\sigma_o)_l^2$ in length units is

$$(\sigma_o)_l^2 = \frac{\left(\sum_{p=1}^{q} l_p\right)^2\left(\sum_{p=1}^{q} h_p d_p l_p r_p^4 \varepsilon_p^2\right)}{\left(\sum_{p=1}^{q} l_p r_p^2 \varepsilon_p\right)^2} \quad (14)$$

The effect of solvent zone length on the calculated zone purity is shown in Fig. 3. It is apparent that the reduction of particle diameter and column length is important to maintain the integrity of the solvent zone. If the minimum acceptable value for the zone purity is arbitrarily defined to be 95%, as illustrated in Fig. 2, the requisite solvent zone length may be determined from Eq. 13 as follows

$$x_j = 80(\sigma_o)_l \quad (15)$$

For example, a solvent zone length greater than 12.7 cm would be required to maintain 95% purity for a column with 5 μm particle diameter and 25 cm length. The limiting zone length given by Eq. 15 is the minimum value that may be used with confidence under the conditions of solvent modulation in order to ensure adherence to the assumptions of the theoretical models.

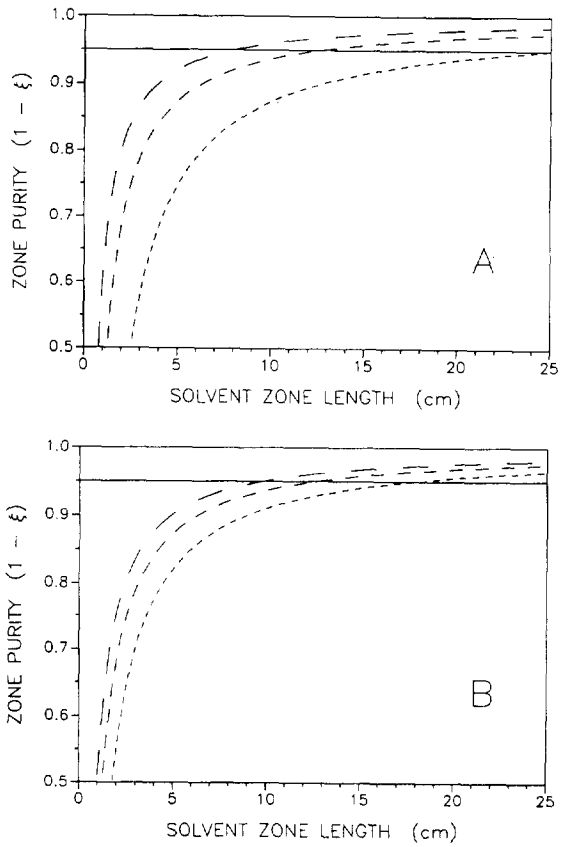

Fig. 3. Effect of solvent zone length on zone purity according to Eqs. 12–14. (A) Constant particle diameter (5 μm) with varying column lengths of 10 cm (——), 25 cm (– –), and 100 cm (---). (B) Constant column length (25 cm) and varying particle diameters of 3 μm (——), 5 μm (– –), and 10 μm (---).

2.4. Optimization strategy

The strategy for optimizing separations requires preliminary measurement of the solute capacity factors in each solvent system on each column to be employed. From these measurements, the retention time and variance can then be predicted by using Eqs. 5 and 10, respectively, for any given solvent zone length and column length in any sequence. After the retention time and variance are calculated for each solute, the extent of separation between adjacent solutes is given by the resolution ($R_{i,i+1}$)

$$R_{i,i+1} = \frac{(T_{i+1} - T_i)}{2[(\sigma_{i+1})_t + (\sigma_i)_t]} \tag{16}$$

The quality of the overall separation is then assessed using a modified form of the multivariate function developed by Schlabach and Excoffier [33], known as the chromatographic resolution statistic (CRS)

$$\mathrm{CRS} = \left[\sum_{i=1}^{m-1}\left(\frac{R_{i,i+1} - R_{\mathrm{opt}}}{R_{i,i+1} - R_{\mathrm{min}}}\right)^2 \cdot \frac{1}{R_{i,i+1}} + \sum_{i=1}^{m-1}\frac{(R_{i,i+1})^2}{(m-1)R_{\mathrm{avg}}^2}\right] \cdot \frac{T_{\mathrm{f}}}{m} \tag{17}$$

where m is the total number of solutes, T_{f} is the elution time of the final solute, R_{opt} is the optimum or desired resolution, R_{min} is the minimum acceptable resolution, and R_{avg} is the average resolution which is given by

$$R_{\mathrm{avg}} = \frac{1}{m} \cdot \sum_{i=1}^{m} R_{i,i+1} \tag{18}$$

The first term of the CRS function is a measure of the extent of separation between each pair of adjacent solute peaks in the chromatogram. This term approaches zero when the individual resolution elements approach the optimum value, and approaches infinity when the individual resolution elements approach the minimum value. The second term of the CRS function reflects the uniformity of spacing between solute peaks, and approaches a minimum value of unity when the sum of the individual resolution elements is equal to the average value. The final term of the CRS function is intended to minimize the analysis time, and may be neglected if this is not a primary goal of the optimization.

In the original expression defined by Schlabach and Excoffier [33], $(R_{i,i+1} - R_{\mathrm{opt}})^2$ passes through a minimum and $1/(R_{i,i+1} - R_{\mathrm{min}})^2$ passes through a maximum as $R_{i,i+1}$ increases. As a result, whenever any individual value of $R_{i,i+1}$ approaches R_{min}, the CRS value becomes extremely high and may no longer be representative of the overall separation quality. More importantly, however, values of $R_{i,i+1}$ that are equidistant from R_{min}, whether higher or lower

in magnitude, are ranked equally. The detrimental consequence is that deceptively low CRS values may be assigned when an individual resolution element approaches zero [34]. This problem may be addressed by altering the form of the CRS function such that, if $R_{i,i+1}$ is less than or equal to $R_{min} + 0.01$, the first term in Eq. 17 is replaced by the constant term

$$\left(\frac{R_{opt} - R_{min}}{0.01}\right)^2 \cdot \frac{1}{R_{min}} \quad (19)$$

In order to optimize the separation, the experimental conditions that yield the minimum value of the CRS function must be determined. The optimum conditions may be determined in two ways: (i) by varying the sequence and length of the solvent zones and columns in a systematic manner to construct a complete CRS response surface, from which the optimum is identified by visual inspection, or (ii) by using an iterative search routine such as the simplex method [19,35].

3. Experimental

3.1. Reagents

Reagent-grade polynuclear aromatic hydrocarbons (PAHs) are obtained from Sigma (St. Louis, MO, USA). Standard solutions are prepared at 10^{-4} M by dissolution of the PAHs in spectroscopic-grade methanol. Organic solvents are high purity distilled-in-glass grade (Baxter Healthcare, Burdick and Jackson Division, Muskegon, MI, USA); water is deionized and doubly distilled in glass (Model MP-3A, Corning Glass Works, Corning, NY, USA).

3.2. Experimental system

The chromatographic system consists of a dual syringe pump (Model 140, Applied Biosystems, San Jose, CA, USA), which is programmed to deliver solvent zones for a specified time period at a nominal flow-rate of 1 μl/min. Sample introduction is achieved by using a 1.0-μl injection valve (Model ECI4W1, Valco Instruments, Houston, TX, USA), after which the effluent stream is split (75:1) and applied to the chromatographic column. The microcolumns are prepared from fused-silica capillary tubing (200 μm I.D., Polymicro Technologies, Phoenix, AZ, USA), whose length can be readily adjusted, which is terminated with a quartz wool frit. The microcolumns are packed with octadecylsilica and β-cyclodextrin silica materials (5 μm diameter, Advanced Separation Technologies, Whippany, NJ, USA) according to the slurry packing procedure described previously [36]. The octadecylsilica and β-cyclodextrin silica columns, respectively, have total porosity (ε_p) of 0.81 and 0.80, separation impedance (ϕ_p) of 890 and 720, and reduced plate height (h_p) of 3.2 and 12.9 using pyrene as a model solute under standard test conditions [36].

The PAH solutes are detected using both laser-induced fluorescence and UV-absorbance in a 75 μm I.D. fused-silica capillary flow cell. In the fluorescence detection system [37,38], a helium–cadmium laser (325 nm, 25 mW, Model 3074-40M, Omnichrome, Chino, CA, USA) is reflected by a dielectric mirror and is focussed on the capillary with a quartz lens. The fluorescence emission is collected perpendicular and coplanar to the excitation beam with another quartz lens, spectrally isolated with a bandpass interference filter (420 nm, S10-420-F, Corion, Holliston, MA, USA), and focussed onto a photomultiplier tube (Model Centronic Q4249B, Bailey Instruments, Saddle Brook, NJ, USA). The photocurrent is amplified and converted to voltage by a picoammeter (Model 480, Keithley Instruments, Cleveland, OH, USA). A variable-wavelength UV-absorbance detector (Model Uvidec 100-V, Japan Spectroscopic Co., Tokyo, Japan), operated at 254 nm, is placed in series after the fluorescence detector. Data are acquired simultaneously from both detectors using an analog-to-digital converter (Model DT2805-5716, Data Translation, Marlborough, MA, USA) together with a personal computer (Model ZMF-248-40, Zenith Data Systems, St. Joseph, MI, USA). The data acquisition programs are written in the Forth-based programming language ASYST

(Version 2.1, Keithley Asyst, Rochester, NY, USA).

3.3. Computer optimization program

The computer optimization program is written in the FORTRAN 77 language to be executed on a VAXstation 3200 computer (Digital Equipment, Maynard, MA, USA). This program generates a complete CRS response surface by using a systematic mapping procedure. The lengths of each column and solvent zone are varied independently within prescribed limits; column lengths are varied from 0 to 75 cm and solvent zones are varied from the minimum length that maintains 95% purity (Eq. 15) to the maximum length required to elute all solutes. For each combination of column and solvent lengths, the total retention time and variance of each solute peak are calculated by means of Eqs. 5 and 10, respectively. The resolution between each pair of adjacent solute peaks is calculated by using Eq.

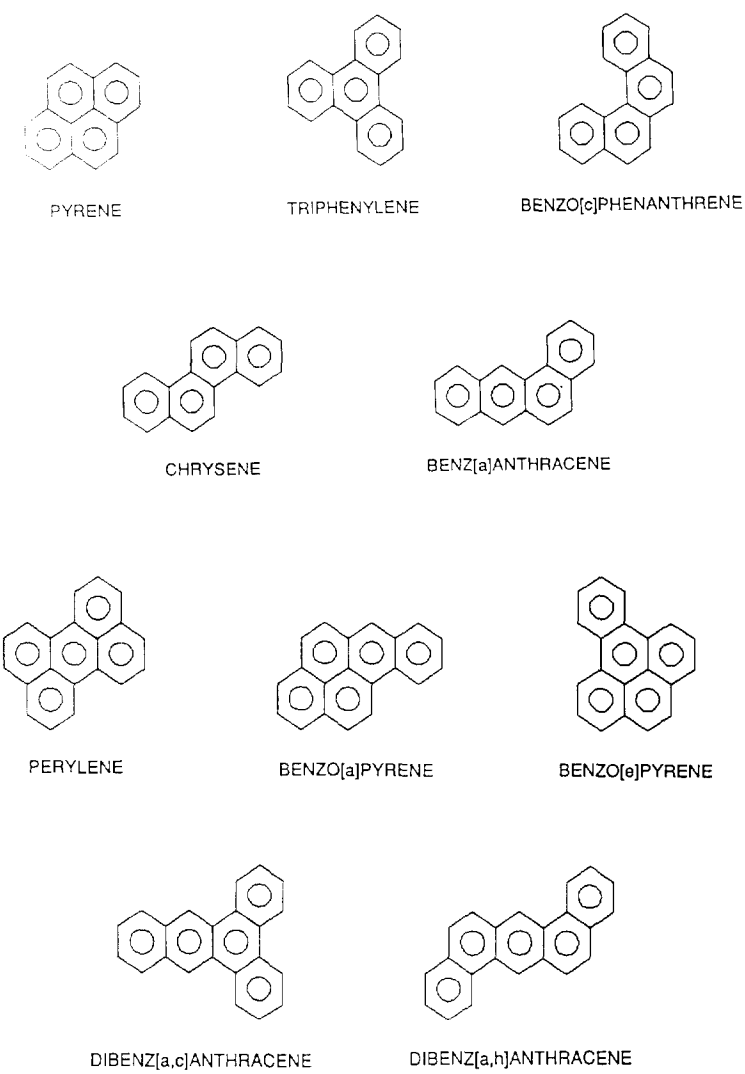

Fig. 4. Structures of isomeric four- and five-ring polynuclear aromatic hydrocarbons.

16. Finally, the overall quality of the separation is assessed by means of the modified CRS function (Eqs. 17 and 19), using selected values for the optimum and minimum acceptable resolution of 1.5 and 0.3, respectively. By graphing the CRS value as a function of the column and solvent zone lengths, a complete multidimensional response surface may be constructed. The minimum CRS value is then identified by visual inspection of the response surface. To assist in identifying the minimum CRS value, the five best conditions are continuously updated and stored in a file by the computer program.

4. Results and discussion

The goal of these preliminary studies is to demonstrate the conceptual basis and to test the theoretical models of solvent modulation using serially coupled columns. To facilitate these goals, the stationary phases were selected for their dissimilar retention mechanisms but compatible mobile phase requirements. Octadecylsilica retains solutes predominantly by a partition mechanism, whereas β-cyclodextrin silica forms inclusion complexes based on the size and shape of the solute. Although both of these phases interact with solutes by Van der Waals forces, monomeric octadecylsilica is dominated by enthalpic effects while β-cyclodextrin silica has a significant entropic contribution. This difference in retention mechanisms may be advantageous for the separation of isomeric four- and five-ring PAHs, whose structures are shown in Fig. 4.

The capacity factors for each PAH were measured on the octadecylsilica and β-cyclodextrin silica stationary phases using mobile phases with compositions of 80% and 90% aqueous methanol as well as 50% and 70% aqueous acetonitrile. On the octadecylsilica phase (Table 1), many of the isomeric four- and five-ring compounds are well separated. However, there are several critical pairs that are difficult to resolve in all mobile phases, most notably chrysene and benz[*a*]anthracene, as well as benzo[*e*]pyrene and perylene.

Table 1
Capacity factors (k_{ijp}) for PAHs on octadecylsilica stationary phase using aqueous methanol and acetonitrile mobile phases

PAH	Capacity factor (k_{ijp})			
	Methanol		Acetonitrile	
	80%	90%	50%	70%
Pyrene	4.65	1.93	14.5	4.12
Triphenylene	5.90	2.39	18.7	5.01
Benzo[*c*]phenanthrene	6.23	2.69	20.9	5.37
Chrysene	6.91	2.61	22.6	5.52
Benz[*a*]anthracene	7.00	2.61	23.0	5.64
Benzo[*e*]pyrene	10.5	3.78	31.8	8.16
Perylene	10.8	3.74	32.0	8.18
Benzo[*a*]pyrene	13.0	4.01	39.3	9.45
Dibenz[*a*,*c*]anthracene	15.0	4.64	49.0	10.6
Dibenz[*a*,*h*]anthracene	17.6	5.45	56.4	11.7

Although PAHs are reported to form inclusion complexes with β-cyclodextrin silica [22,39–42], the capacity factors are very small under all experimental conditions examined herein (Table 2). Only by using the weakest mobile phases is the PAH retention measurable and the resolution partially achieved. Although methanol mobile phases show no selectivity based on either solute size or shape, the acetonitrile mobile

Table 2
Capacity factors (k_{ijp}) for PAHs on β-cyclodextrin silica stationary phase using aqueous methanol and acetonitrile mobile phases

PAH	Capacity factor (k_{ijp})			
	Methanol		Acetonitrile	
	80%	90%	50%	70%
Pyrene	0.09	0.06	0.18	0.08
Triphenylene	0.11	0.06	0.16	0.08
Benzo[*c*]phenanthrene	0.13	0.06	0.18	0.07
Chrysene	0.15	0.07	0.17	0.08
Benz[*a*]anthracene	0.15	0.06	0.19	0.09
Benzo[*e*]pyrene	0.12	0.06	0.25	0.14
Perylene	0.18	0.14	0.36	0.17
Benzo[*a*]pyrene	0.15	0.07	0.26	0.15
Dibenz[*a*,*c*]anthracene	0.16	0.08	0.35	0.16
Dibenz[*a*,*h*]anthracene	0.18	0.08	0.37	0.17

phases appear to be able to discriminate between the four- and five-ring classes. The most noteworthy and useful result is that perylene may be readily separated from both benzopyrene isomers on the β-cyclodextrin silica phase.

Based on these results, it seems reasonable to expect that resolution of the PAHs can be achieved by serial coupling of the octadecylsilica and β-cyclodextrin silica columns. However, there are 64 possible permutations for the columns and solvents examined in this study: 8 one-column/one-solvent systems, 24 one-column/two-solvent systems, 8 two-column/one-solvent systems, and 24 two-column/two-solvent systems. It would clearly be impossible to examine all of these possibilities by time-consuming, trial-and-error experimental measurements. However, the computer program described previously provides a rapid and effective means to identify the most promising permutation. The individual capacity factors (k_{ijp}) for the PAH solutes shown in Tables 1 and 2 are used to calculate the retention time and variance according to Eqs. 5 and 10, respectively. The resolution of each adjacent pair of solutes is calculated from Eq. 16, and the overall quality of the separation is assessed by the CRS function in Eq. 17. For each possible combination and sequence of columns and solvents, the minimum CRS values are stored in a file and are used to identify the most promising permutation for further study. The results of these preliminary simulations are summarized in Table 3 for the permutations of a two-column/two-solvent chromatographic system. If the minimum CRS value is used as the criterion for evaluation, then the best column sequence is predicted to be octadecylsilica followed by β-cyclodextrin silica, and the best solvent sequence is 80% methanol followed by 50% acetonitrile. These conditions should provide a minimum resolution of 0.97 with a total analysis time of 113 min.

If resolution and not analysis time is considered to be the primary goal, the final term may be neglected in evaluation of the CRS function in Eq. 17. Under these conditions, the results for the permutations of a two-column/two-solvent chromatographic system are summarized in Table 4. In some cases, the optimum separation is virtually identical to that identified in Table 3; in other cases, a significant increase in resolution is achieved, usually at the expense of an increase in analysis time. Again, the most promising choice for column sequence is octadecylsilica followed by β-cyclodextrin silica, and the most promising solvent sequence is 80% methanol

Table 3
Evaluation of the permutations of a two-column/two-solvent chromatographic system for the separation of PAHs

Column 1	Column 2	Solvent 1	Solvent 2	T_f (min)	$(R_{i,i+1})_{min}$	CRS_{min}
ODS	β-CD	80% CH_3OH	90% CH_3OH	326	0.61	520
ODS	β-CD	90% CH_3OH	80% CH_3OH	373	0.61	590
ODS	β-CD	50% CH_3CN	70% CH_3CN	349	0.71	250
ODS	β-CD	70% CH_3CN	50% CH_3CN	344	0.72	250
ODS	β-CD	80% CH_3OH	50% CH_3CN	113	0.97	33
ODS	β-CD	50% CH_3CN	80% CH_3OH	159	0.99	43
ODS	β-CD	80% CH_3OH	70% CH_3CN	326	0.85	160
ODS	β-CD	70% CH_3CN	80% CH_3OH	318	0.87	160
ODS	β-CD	90% CH_3OH	50% CH_3CN	282	0.59	530
ODS	β-CD	50% CH_3CN	90% CH_3OH	259	0.59	480
ODS	β-CD	90% CH_3OH	70% CH_3CN	241	0.46	3,100
ODS	β-CD	70% CH_3CN	90% CH_3OH	209	0.48	2,500

The columns are octadecylsilica (ODS) and β-cyclodextrin silica (β-CD); the solvents are aqueous mixtures of methanol (CH_3OH) and acetonitrile (CH_3CN) as given in Tables 1 and 2. The analysis time (T_f), minimum resolution [$(R_{i,i+1})_{min}$] and minimum chromatographic resolution statistic (CRS_{min}) function corresponding to the optimum conditions are given.

Table 4
Evaluation of the permutations of a two-column/two-solvent chromatographic system for the separation of PAHs

Column 1	Column 2	Solvent 1	Solvent 2	T_f (min)	$(R_{i,i+1})_{min}$	CRS_{min}
ODS	β-CD	80% CH_3OH	90% CH_3OH	374	0.61	16
ODS	β-CD	90% CH_3OH	80% CH_3OH	373	0.61	16
ODS	β-CD	50% CH_3CN	70% CH_3CN	349	0.71	7.3
ODS	β-CD	70% CH_3CN	50% CH_3CN	344	0.72	7.2
ODS	β-CD	80% CH_3OH	50% CH_3CN	666	1.39	1.9
ODS	β-CD	50% CH_3CN	80% CH_3OH	586	1.37	2.0
ODS	β-CD	80% CH_3OH	70% CH_3CN	326	0.85	5.0
ODS	β-CD	70% CH_3CN	80% CH_3OH	322	0.87	5.0
ODS	β-CD	90% CH_3OH	50% CH_3CN	427	0.70	15
ODS	β-CD	50% CH_3CN	90% CH_3OH	386	0.70	15
ODS	β-CD	90% CH_3OH	70% CH_3CN	241	0.46	130
ODS	β-CD	70% CH_3CN	90% CH_3OH	209	0.48	120

The columns are octadecylsilica (ODS) and β-cyclodextrin silica (β-CD); the solvents are aqueous mixtures of methanol (CH_3OH) and acetonitrile (CH_3CN) as given in Tables 1 and 2. The analysis time (T_f), minimum resolution $[(R_{i,i+1})_{min}]$ and minimum chromatographic resolution statistic (CRS_{min}) function corresponding to the optimum conditions are given, when analysis time is not considered to be a goal of the optimization.

followed by 50% acetonitrile. This permutation will be evaluated in further detail below.

In order to identify the most favorable experimental conditions, the computer program is used first to determine the optimum lengths of the octadecylsilica and β-cyclodextrin silica columns. The topographic and contour maps of the CRS response surface are shown in Fig. 5 as a function of the column length. It is apparent that the overall quality of the separation improves dramatically with increasing length of the octadecylsilica column. Although the extent of the

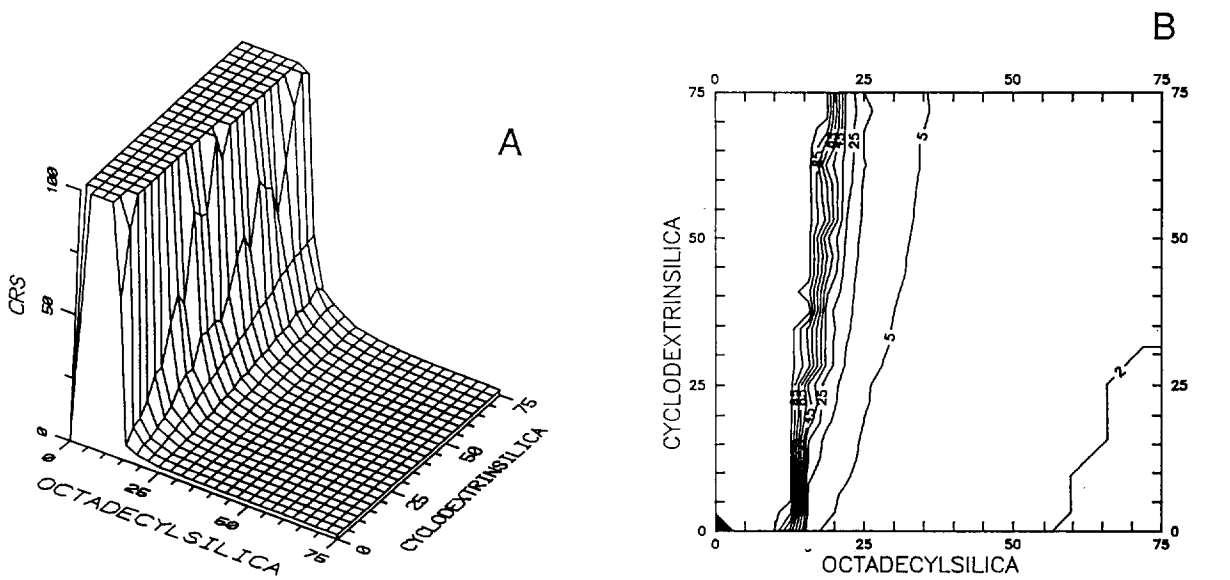

Fig. 5. Topographic (A) and contour (B) maps of the CRS response surface as a function of the column length (cm) for octadecylsilica and β-cyclodextrin silica.

improvement after 25 cm is relatively small, the minimum CRS value is achieved for a column length of 75 cm. In contrast, the β-cyclodextrin silica column has no beneficial effect upon the separation and, thus, has an optimal column length of 0 cm.

The computer program is used next to determine the optimum lengths of the 80% methanol and 50% acetonitrile solvent zones. The topographic and contour maps of the CRS response surface are shown in Fig. 6 as a function of the solvent zone length. There are several regions that yield low values for the CRS function; the overall minimum value is observed for solvent lengths of 167 cm of 80% methanol and 318 cm of 50% acetonitrile.

The predicted separation of the isomeric four- and five-ring PAHs with a 75-cm octadecylsilica column is shown in Fig. 7. The optimal solvent modulation sequence of 80% methanol and 50% acetonitrile in zones of 167 and 318 cm length, respectively, provides a good overall separation (CRS = 1.9) with an analysis time of 666 min. Under these conditions, the critical solute pair is chrysene and benz[*a*]anthracene ($R_{i,i+1} = 1.39$). All other solute pairs have resolution greater than the optimum value (1.5), which is desirable for accurate qualitative and quantitative analysis.

Although this optimized separation initially appears to be very promising, a more detailed examination of the CRS response surfaces is warranted. In the immediate vicinity of the optimum conditions shown in Fig. 6, the CRS function is found to vary in a significant and abrupt manner. For example, as the solvent zone length of 80% methanol changes by ±5 cm, the

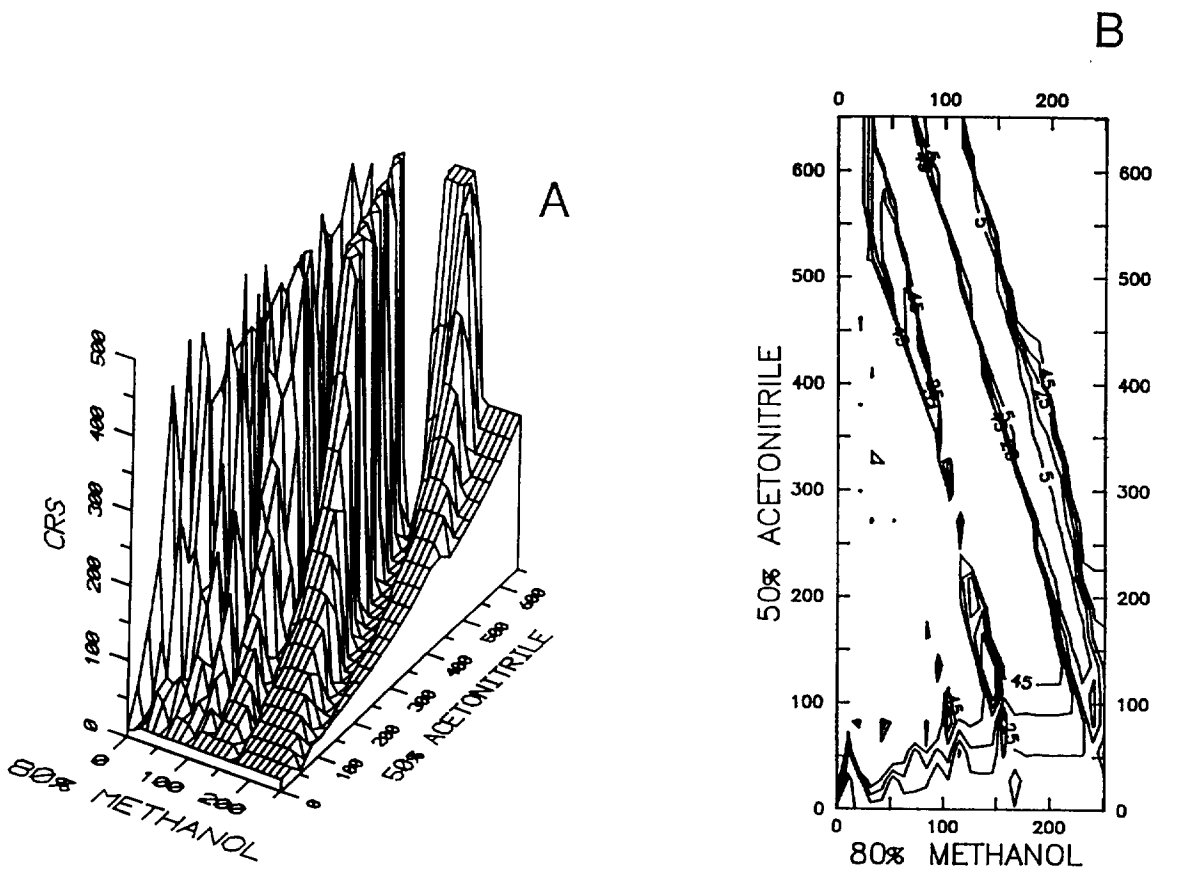

Fig. 6. Topographic (A) and contour (B) maps of the CRS response surface as a function of the solvent zone length (cm) for 80% methanol and 50% acetonitrile.

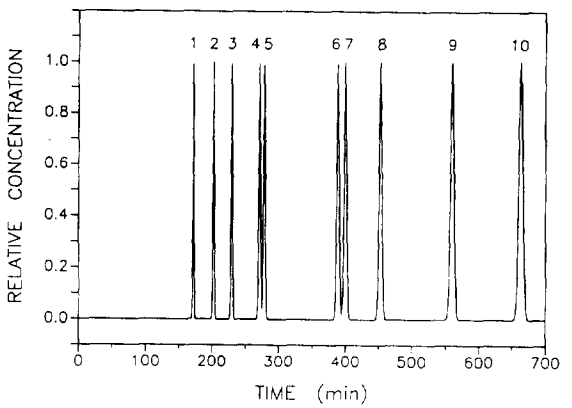

Fig. 7. Predicted chromatogram for the isomeric PAHs with a 75-cm octadecylsilica column using the optimal solvent modulation sequence of 80% methanol and 50% acetonitrile in zones of 167 and 318 cm length, respectively. Solutes: 1 = pyrene; 2 = triphenylene; 3 = benzo[*c*]phenanthrene, 4 = chrysene; 5 = benz[*a*]anthracene; 6 = benzo[*e*]pyrene; 7 = perylene; 8 = benzo[*a*]pyrene; 9 = dibenz[*a,c*]anthracene; 10 = dibenz[*a,h*]anthracene.

CRS value increases by approximately two orders of magnitude. Thus, small variations in the experimental conditions may have a highly detrimental effect upon the quality of the separation. The next most favorable permutation identified from Table 4, in which the column sequence is octadecylsilica followed by β-cyclodextrin silica and the solvent sequence is 70% acetonitrile followed by 80% methanol, does not suffer from this limitation. This permutation will be evaluated in further detail below.

The topographic and contour maps of the CRS response surface are shown in Fig. 8 as a function of the column length. The overall quality of the separation improves continuously with increasing length of the octadecylsilica column, up to the limit of 75 cm. As noted for the previous case, β-cyclodextrin silica is relatively ineffectual and, thus, has an optimal length of 0 cm.

The topographic and contour maps of the CRS response surface are shown in Fig. 9 as a function of the solvent zone length. There is a broad region of the surface having relatively low values for the CRS function; the minimum value is achieved for solvent lengths of 203 cm of 70% acetonitrile and 634 cm of 80% methanol.

The predicted separation of the isomeric four- and five-ring PAHs with a 75-cm octadecylsilica column is shown in Fig. 10. The optimal solvent modulation sequence of 70% acetonitrile and 80% methanol in zones of 203 and 634 cm length, respectively, provides an excellent sepa-

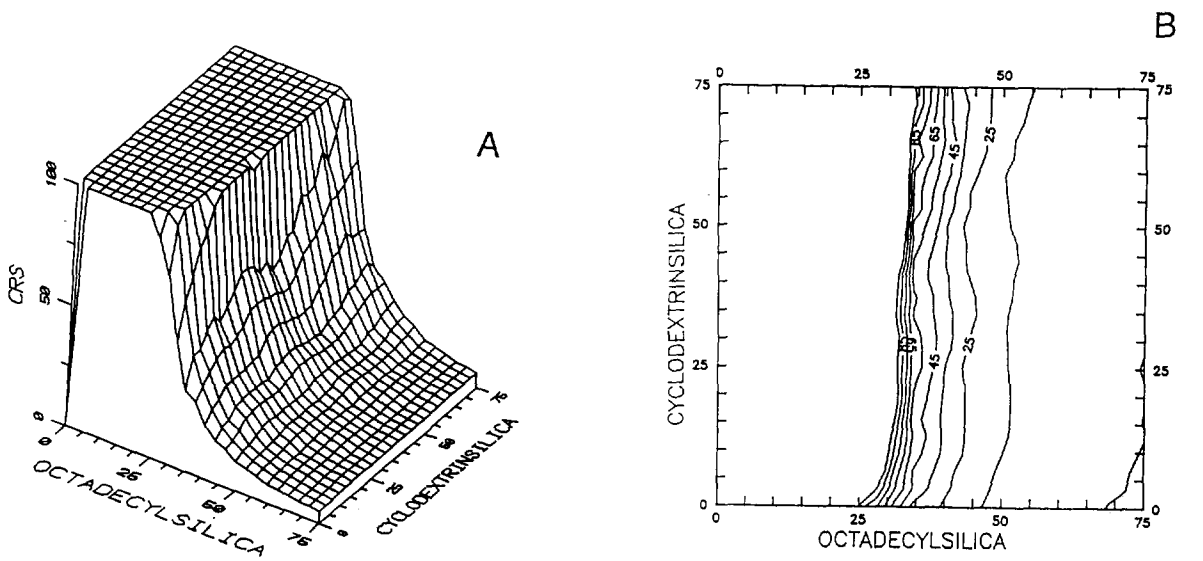

Fig. 8. Topographic (A) and contour (B) maps of the CRS response surface as a function of the column length (cm) for octadecylsilica and β-cyclodextrin silica.

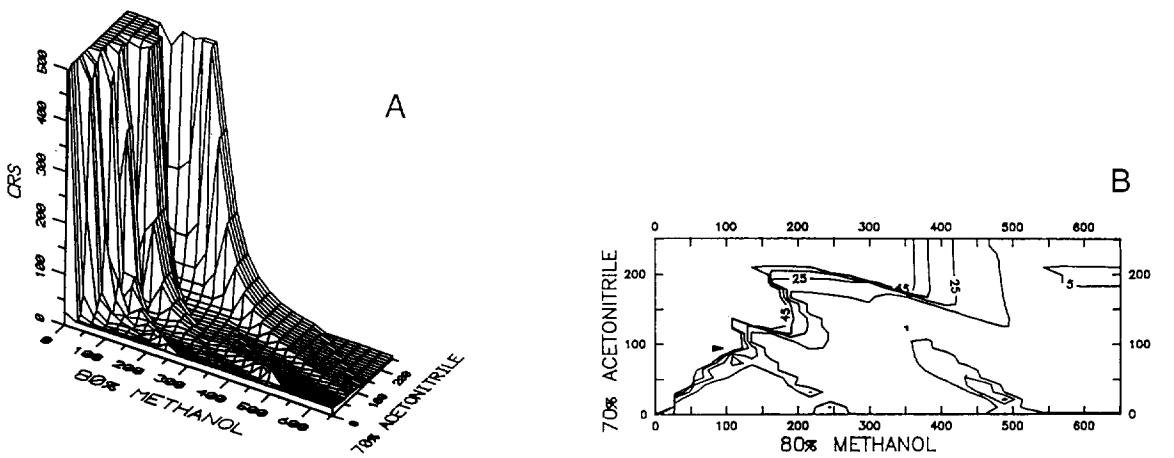

Fig. 9. Topographic (A) and contour (B) maps of the CRS response surface as a function of the solvent zone length (cm) for 70% acetonitrile and 80% methanol.

ration (CRS = 5.0) with an analysis time of 320 min. All solute pairs have resolution greater than the minimum acceptable value (0.3), whereas two pairs have resolution less than the optimum value (1.5). These critical solute pairs are chrysene and benz[*a*]anthracene ($R_{i,i+1} = 0.88$), as well as benzo[*e*]pyrene and perylene ($R_{i,i+1} = 0.88$). Because the CRS response surfaces shown in Figs. 8 and 9 are relatively flat in the vicinity of the optimum, small discrepancies in column length and solvent zone length should have little effect upon the quality of the separation. Thus, the analytical method should be relatively reproducible and rugged.

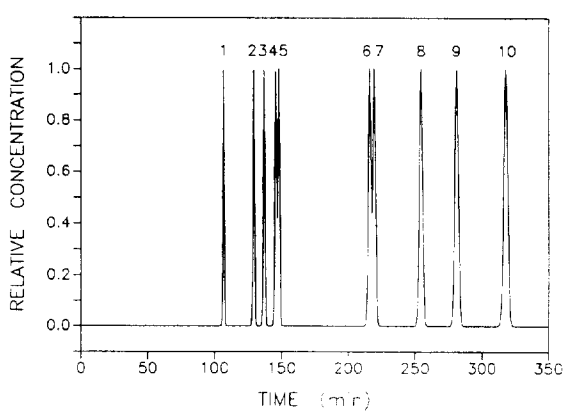

Fig. 10. Predicted chromatogram for the isomeric PAHs with a 75-cm octadecylsilica column using the optimal solvent modulation sequence of 70% acetonitrile and 80% methanol in zones of 203 and 634 cm length, respectively. Solutes as given in Fig. 7.

In order to demonstrate the practical application of this method, the separation of the isomeric four- and five-ring PAHs was performed under the predicted optimum conditions. The experimental chromatogram (Fig. 11) shows excellent separation of all PAH standards with resolution comparable to that in the predicted chromatogram (Fig. 10). The experimental retention time and peak width for each PAH standard agree well with the theoretically predicted values from Eqs. 5 and 10, respectively, as summarized in Table 5. The average relative error is ±3.5% for retention time and ±21% for peak width. Thus, the theoretical models developed herein can accurately predict the experimental results for solvent modulation in serially coupled columns.

5. Conclusions

The complete optimization of separations in multimodal or multidimensional liquid chromatography is a non-trivial task due, in part, to the large number of variable parameters and, in part, to deviations from ideal retention behavior. The use of serially coupled columns with solvent

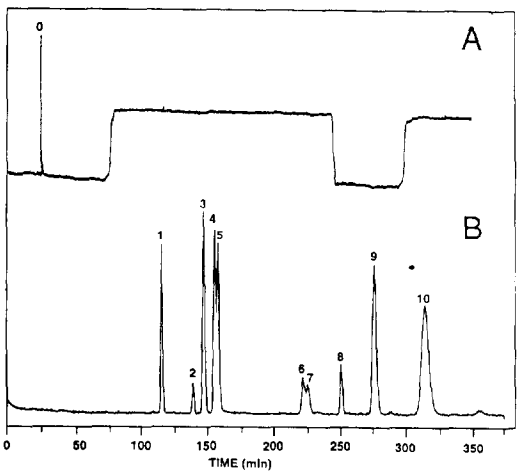

Fig. 11. Experimental chromatogram obtained under the predicted optimum conditions. Column: 75 cm × 200 μm I.D. fused-silica capillary, packed with 5 μm octadecyl silica. Mobile phase: solvent modulation sequence of 70% acetonitrile and 80% methanol in zones of 203 and 634 cm length, respectively, 0.95 μl/min. Detectors: (A) UV–visible absorbance at 254 nm to indicate solvent modulation sequence, (B) Laser-induced fluorescence with excitation at 325 nm and emission at 420 nm to indicate solute retention. Solutes: 0 = injection solvent; 1 = pyrene; 2 = triphenylene; 3 = benzo[*c*]phenanthrene; 4 = chrysene; 5 = benz[*a*]anthracene; 6 = benzo[*e*]pyrene; 7 = perylene; 8 = benzo[*a*]pyrene; 9 = dibenz[*a*,*c*]anthracene; 10 = dibenz[*a*,*h*]anthracene.

modulation appears to be a promising approach to this problem. Because the individual stationary and mobile phases are spatially separated from one another, solute retention is a simple, time-weighted average of each environment to which the solute is exposed. For a system comprised of q columns and n solvents, only $q \times n$ measurements of the solute capacity factor are necessary. From these measurements, retention may be accurately predicted for any sequence and length of the stationary and mobile phases. This approach was demonstrated for the separation of isomeric polynuclear aromatic hydrocarbons using octadecylsilica and β-cyclodextrin silica stationary phases with aqueous methanol and acetonitrile mobile phases. Based on these results, this approach appears to be a viable strategy for the simultaneous optimization of stationary and mobile phase environments.

Acknowledgements

The authors are grateful to Thomas E. Beesley (Advanced Separation Technologies) for providing the octadecylsilica and β-cyclodextrin silica

Table 5
Comparison of experimental (Expt) and theoretical (Theory) retention time and peak width under the predicted optimum conditions illustrated in Figs. 10 and 11

PAH	Retention time (min)			Width (min)		
	Expt	Theory[a]	Error (%)[b]	Expt	Theory[c]	Error (%)[b]
Pyrene	112	107	4.7	2.3	2.0	15
Triphenylene	136	129	5.4	2.8	2.4	17
Benzo[*c*]phenanthrene	143	137	4.4	3.0	2.5	20
Chrysene	151	146	3.4	3.1	2.7	15
Benz[*a*]anthracene	154	148	4.1	3.1	2.7	15
Benzo[*e*]pyrene	218	217	0.5	3.2	4.0	−20
Perylene	221	220	0.5	3.2	4.1	−22
Benzo[*a*]pyrene	247	257	−3.9	4.1	4.8	−15
Dibenz[*a*,*c*]anthracene	271	284	−4.6	5.1	5.2	−6.0
Dibenz[*a*,*h*]anthracene	310	320	−3.1	9.9	5.9	68
Average			±3.5			±21

[a] Calculated from Eq. 5.
[b] Error (%) = 100 (Expt − Theory)/Theory.
[c] Calculated from Eq. 10, assuming a peak width of $4(\sigma_t)_i$.

stationary phases, and to Matthew Bosma (Baxter Healthcare) for providing high-purity solvents. This research was supported by the US Department of Energy, Office of Basic Energy Sciences, Division of Chemical Sciences, under contract number DE-FG02-89ER14056.

References

[1] Cs. Horváth, W. Melander and I. Molnár, *J. Chromatogr.*, 125 (1976) 129.
[2] P. Jandera, H. Colin and G. Guiochon, *Anal. Chem.*, 54 (1982) 435.
[3] S.T. Balke, *Quantitative Column Liquid Chromatography: A Survey of Chemometric Methods* (*Journal of Chromatogr. Library*, Vol. 29), Elsevier, Amsterdam, 1984.
[4] J.C. Berridge, *Techniques for the Automated Optimization of HPLC Separations*, Wiley, New York, 1985.
[5] P.J. Schoenmakers, *Optimization of Chromatographic Selectivity* (*Journal of Chromatogr. Library*, Vol. 35), Elsevier, Amsterdam, 1986.
[6] J.L. Glajch and L.R. Snyder, *Computer-Assisted Method Development for High-Performance Liquid Chromatography*, Elsevier, Amsterdam, 1990.
[7] J.L. Glajch, J.J. Kirkland, K.M. Squire and J.M. Minor, *J. Chromatogr.*, 199 (1980) 57.
[8] J.W. Dolan, L.R. Snyder and M.A. Quarry, *Chromatographia*, 24 (1987) 261.
[9] S.J. Costanzo, *J. Chromatogr. Sci.*, 24 (1986) 89.
[10] G.J. Janz and R.P.T. Tomkins, *Nonaqueous Electrolyte Handbook*, Volume 1, Academic Press, New York, 1972.
[11] H. Colin, G. Guiochon and P. Jandera, *Anal. Chem.*, 55 (1988) 442.
[12] V.V. Berry, *J. Chromatogr.*, 321 (1985) 33.
[13] V.V. Berry and R.W. Shansky, *J. Chromatogr.*, 284 (1984) 303.
[14] V.V. Berry, *J. Chromatogr.*, 290 (1984) 143.
[15] J.C. Gluckman, K. Slais, U.A.T. Brinkman and R.W. Frei, *Anal. Chem.*, 59 (1987) 79.
[16] E.L. Little, M.S. Jeansonne and J.P. Foley, *Anal. Chem.*, 63 (1991) 33.
[17] J.H. Wahl, C.G. Enke and V.L. McGuffin, *Anal. Chem.*, 62 (1990) 1416.
[18] J.H. Wahl, C.G. Enke and V.L. McGuffin, *Anal. Chem.*, 63 (1991) 1118.
[19] J.H. Wahl and V.L. McGuffin, *J. Chromatogr.*, 485 (1989) 541.
[20] I.H. Hagestam and T.C. Pinkerton, *Anal. Chem.*, 57 (1985) 1757.
[21] C.P. Desilets, M.A. Rounds and F.E. Regnier, *J. Chromatogr.*, 544 (1991) 25.
[22] H.J. Issaq, D.W. Mellini and T.E. Beesley, *J. Liq. Chromatogr.*, 11 (1988) 333.
[23] B. Feibush and C.T. Santasania, *J. Chromatogr.*, 544 (1991) 41.
[24] J.B. Crowther and R.A. Hartwick, *Chromatographia*, 16 (1982) 349.
[25] R. Bischoff and L.W. McLaughlin, *J. Chromatogr.*, 270 (1983) 117.
[26] L.A. Kennedy, W. Kopaciewicz and F.E. Regnier, *J. Chromatogr.*, 359 (1986) 73.
[27] Z. El Rassi and Cs. Horváth, *J. Chromatogr.*, 359 (1986) 255.
[28] H.J. Issaq and J. Gutierrez, *J. Liq. Chromatogr.*, 11 (1988) 2851.
[29] D.J. Pietrzyk, S.M. Senne and D.M. Brown, *J. Chromatogr.*, 546 (1991) 101.
[30] J.H. Wahl, *Ph.D. dissertation*, Michigan State University, East Lansing, MI, 1991.
[31] J.C. Giddings, *Dynamics of Chromatography*, Marcel Dekker, New York, 1965.
[32] J.C. Sternberg, *Adv. Chromatogr.*, 2 (1966) 205.
[33] T.D. Schlabach and J.L. Excoffier, *J. Chromatogr.*, 439 (1988) 173.
[34] M.F.M. Tavares and V.L. McGuffin, *Anal. Chem.*, in press.
[35] S.N. Deming and S.L. Morgan, *Anal. Chem.*, 45 (1973) 278A.
[36] J.C. Gluckman, A. Hirose, V.L. McGuffin and M. Novotny, *Chromatographia*, 17 (1983) 303.
[37] V.L. McGuffin and R.N. Zare, *Appl. Spectrosc.*, 39 (1985) 847.
[38] M.A. Heindorf and V.L. McGuffin, *J. Chromatogr.*, 464 (1989) 186.
[39] D.W. Armstrong, W. DeMond, A. Alak, W.L. Hinze, T.E. Riehl and K.H. Bui, *Anal. Chem.*, 57 (1985) 234.
[40] D.W. Armstrong, A. Alak, W. DeMond, W.L. Hinze and T.E. Riehl, *J. Liq. Chromatogr.*, 8 (1985) 261.
[41] M. Olsson, L.C. Sander and S.A. Wise, *J. Chromatogr.*, 477 (1989) 277.
[42] P.R. Fielden and A.J. Packham, *J. Chromatogr.*, 516 (1990) 355.